Chiang Mai J. Sci. 2020; 47(3) : 598-606
http://epg.science.cmu.ac.th/ejournal/
Contributed Paper

Stress Analysis of Various Shaped PMMA Using Babinet Compensator in Reflection Polariscope

Yongyut Manjit [a], Chanokporn Chaiwong [b], Apichart Limpichaipanit [b,c] and Athipong Ngamjarurojana*[b,c]

[a] Faculty of Science at Si Racha, Kasetsart University Si Racha Campus, Chon Buri 20230, Thailand.

[b] Department of Physics and Materials Science, Faculty of Science, Chiang Mai University, Chiang Mai 50200, Thailand.

[c] Research Center in Physics and Astronomy, Faculty of Science, Chiang Mai University, Chiang Mai 50200, Thailand.

*Author for correspondence; e-mail: ngamjarurojana@yahoo.com

Received: 11 September 2019
Revised: 20 October 2019
Accepted: 30 October 2019

ABSTRACT

The induced stress relations of PMMA (Poly methyl methacrylate) were investigated by two-point loading of hydraulic press system at top and bottom 535.4, 688.6, 841.6 and 994.6 N of various shapes in square, octagon, dodecagon and circular disk. All of samples had the same diagonal length and thickness of 2.5 and 0.6 cm respectively. We observed the number of fringe order of isochromatic fringe pattern at first quadrant of sample by using Babinet compensator in reflection polariscope. The net number of fringe order was used to calculate the relative maximum number of fringe order in horizontal direction of sample by equation of N_{max} - N_i. And this parameter was used to analyze the stress distribution in samples. It was found that the dark band could be observed at the edge of first straight edge of square, octagon and dodecagon shape but dark band did not appear on the edge of disk. The maximum fringe orders of octagon, dodecagon and circular disk at X/R = 0.0, Y/R = 0.9 were 15 fringe orders and the maximum fringe order of square at X/R = 0.0, Y/R = 0.8 was 8.81 fringe orders. Fringe order at contact area decreased along vertical direction and minimum fringe orders at X/R = 0.5, Y/R = 0.0 of square, octagon, dodecagon and circular disk were 3.53, 3.35, 2.62 and 3.72 fringe orders respectively. The relative number of fringe order of square was more than octagon and dodecagon. It means that the transmission of stress in horizontal direction of square was more than octagon and dodecagon.

Keywords: stress analysis, reflection photoelasticity, babinet compensator, various shapes

1. INTRODUCTION

Photoelasticity is an experimental method to observe full-field of stress model [1-3] and it utilizes the relationship between the polarization of light and birefringent behavior to determine stress-strain distribution of materials. The arrangements set-up in photoelasticity consist of light source and polariscope system, hydraulic press system and camera system as shown in Figure 1. The

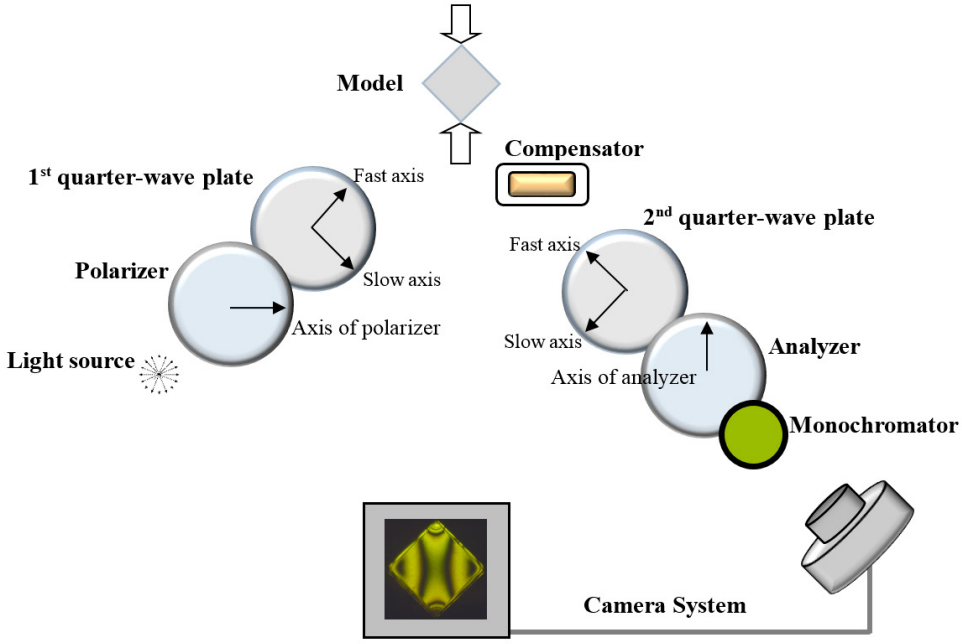

Figure 1. Arrangement of the reflection photoelastic setup.

polariscope system is used to convert unpolarized light from light source to plane or circular polarized light to observe the isoclinic and isochromatic fringes patterns in every point of sample [4]. In the experiment of photoelasticity, the unpolarized light travels through the first polarizer and a first quarter-wave plate to produce the polarized light. The polarized light travels through sample and reflects from surface of sample travels back through second quarter wave-plate and analyzer and observed the fringe patterns are observed by camera system [5-6]. Furthermore, we use these patterns to calculate and analyze the stress and strain in materials using numerical methods or stress-strain optic laws [7-9].

The elasticity of material depends on temperature, structure, size or shape of material. There are many variables related to deformation and elasticity of materials. Stress is one of the parameters and we can analyze the deformation in the material by using the photoelasticity because this experiment method can analyze the stress at local area in the model. This research will focus on the investigation of the stress distribution with various shaped Poly(methyl methacrylate), PMMA [10] compressed by two-point loading of hydraulic press system and the observation of the isochromatic fringe pattern of PMMA using reflection polariscope. Sample shapes for the stress distribution investigation consist of square, octagon, dodecagon and circular disk. The diagonal length and thickness were 2.5 and 0.6 cm respectively and the compressive force was varied as 535.4, 688.6, 841.6 and 994.6 N. In this experiment we added the compensator into the basic reflection polariscope to observe the integer and fractional number of isochromatic fringe order at first quadrant in each sample and then the results were used to calculate the relative maximum number of fringe order in horizontal direction to compare the effect of shapes on stress distribution in PMMA samples.

2. MATERIALS AND METHOD

In this research, we observed the isochromatic fringe pattern of various shapes of PMMA consisting

of circular disk, square, octagon and dodecagon. In this experiment we compressed the sample by hydraulic press system, and we measured the magnitude of force by adding the load cell into the hydraulic press system. The change of load cell voltage depended on magnitude of compressive force and the linear relation between force and voltage is 7.65 N/mV.

We adjusted the axis of first and second of polarizer and quarter-wave plate that was circular polariscope in this experiment to observe the isochromatic fringe pattern [11]. The number of isochromatic fringe order was observed on any co-ordinate (x,y) point of circular disk where x = X/R = 0, 0.1, 0.2,…in horizontal direction and y = Y/R = 0, 0.1, 0.2, … in vertical direction (R is radius of disk, X,Y are co-ordination in x-y plane) at first quadrant of sample where the grids were drawn by computer program. We added the Babinet compensator to the basic circular reflection polariscope to observe the integer and fractional number fringe order of isochromatic fringe pattern [12].

Isochromatic fringe pattern on model was related with the change of knob scale compensator. In experiment, we found the value of knob scale compensator in one cycle of isochromatic fringe patter on model (x). Next, we found the value of knob scale (y) which was adjusted until the dark band isochromatic fringe pattern cross at interest point. These values were used to calculate the fractional number of isochromatic fringe order in equation r = y/x. Finally, we calculated the net number of isochromatic fringe order (N) with equation (1) that is the combination of integer (n) and fractional isochromatic fringe order [13]:

$$N = n \pm r \quad (1)$$

The total number of isochromatic fringe order used to calculate the relative maximum number of isochromatic fringe order in each grid point of sample is shown in equation (2):

Relative maximum number of fringe order

$$= N_{max} - N_i \quad (2)$$

where N_i is number of fringe order at every position in horizontal direction of sample

N_{max} is maximum number of fringe order in each along horizontal direction

In this research, we calculated the relative maximum number of isochromatic fringe order in horizontal direction of samples, which was the parameter related to the transmission of force or stress distribution in horizontal direction of samples. In case of high value of relative maximum number of fringe order, the transmission of force or stress distribution in horizontal direction was low from position of maximum number of fringe order to each point in horizontal of sample. Nevertheless, in case of low value of relative maximum number of fringe order, the transmission of force or stress distribution in horizontal direction was high from position of maximum number of fringe order to each point in horizontal of sample.

3. RESULTS AND DISCUSSION

3.1 Effect of Various Shaped Sample with Stress Distribution in Horizontal Direction

The results in this part are the isochromatic fringe pattern of four shapes of samples, namely square, octagon, dodecagon and circular disk. In each shape of sample, two-point loading at top and bottom was applied and the magnitude of force was 535.4, 688.6, 841.6 and 994.6 N. The isochromatic fringe patterns were dark band of isochromatic fringe patterns cross on any co-ordinate (x,y) point of disk. We rotated the knob of compensator until dark band cross co-ordinate (x,y) point and this value of rotating compensator scale was used to calculate total fringe order. It was found that fringe order depended on shape edge of sample. The fringe order of curve edge of circular disk was more than straight edge of square, octagon and dodecagon shape because of greater edge length. The transmission of force from contact area to center in vertical direction

of curve edge of circular disk was more than straight edge of square, octagon and dodecagon shape because of the distribution of force to the nearest edge of sample. Fringe order of square was more than octagon and dodecagon because of less interior angle and hence more distribution of force in vertical direction to the edge and every point of sample.

Figures. 2-5. show the relative maximum number of fringe order of PMMA in square, octagon, dodecagon and circular disk shape [14]. The relative maximum number of fringe order in each position at X/R was calculated from the difference between the value of maximum number of fringe order at X/R = 0 and the number of fringe order in each position at X/R. We compared the relative maximum number of fringe order of different of magnitude of force consisting of 535.4, 688.6, 841.6 and 994.6 N. It was found that the transmission of force from contact area to vertical direction X/R=0 of sample was more than another region. Fringe order at vertical direction of disk increased, which was related to the force increase more than increasing of fringe order at another region of disk. Therefore, the relative maximum number of fringe order increased as magnitude of force increased in every shape of PMMA. The transmission of force from position of X/R = 0

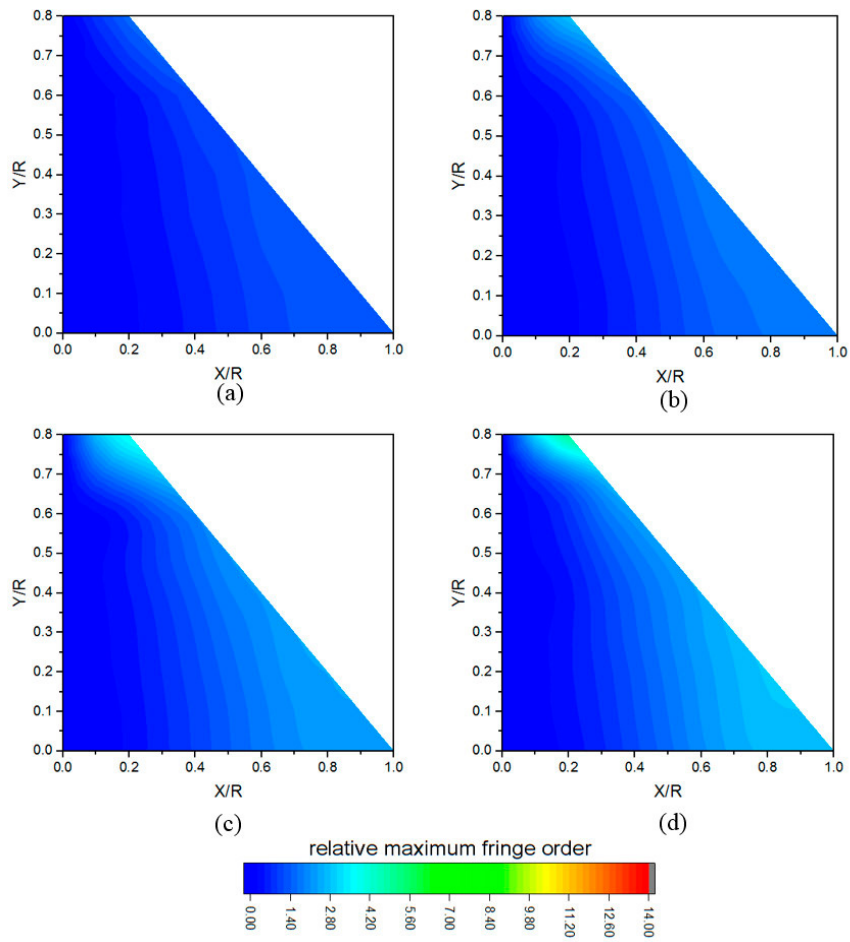

Figure 2. Relative maximum number of fringe order with X/R and Y/R of square shape and magnitude of load (a) 535.4 N (b) 688.6 N (c) 841.6 N (d) 994.6 N.

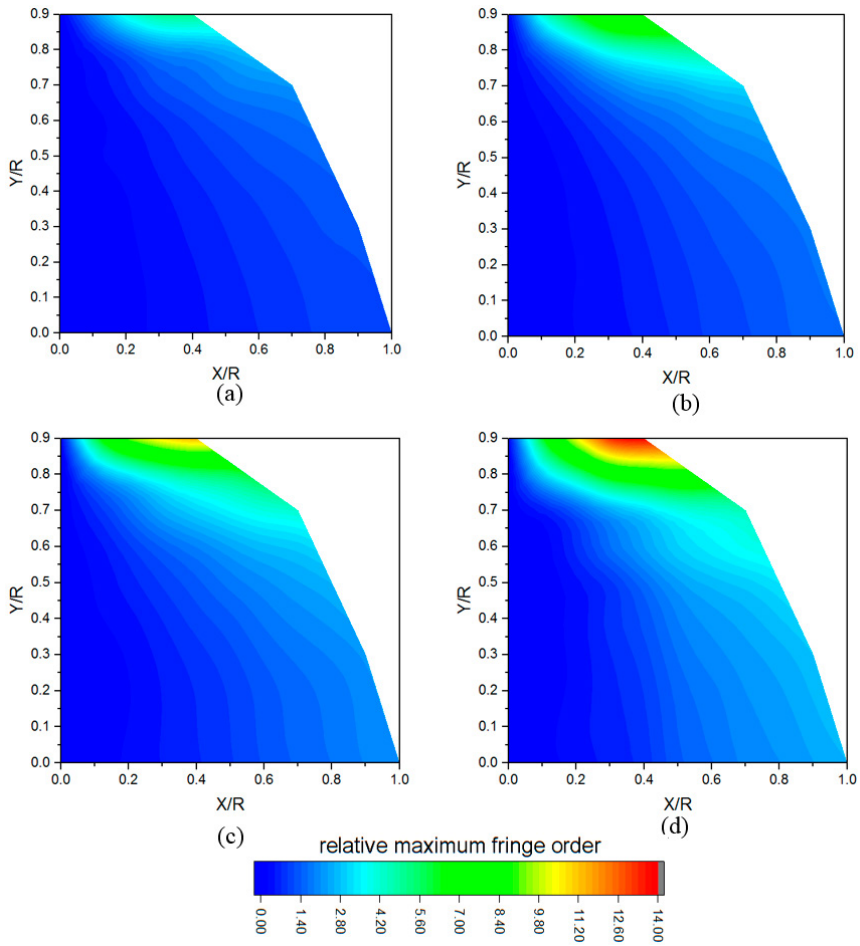

Figure 3. Relative maximum number of fringe order with X/R and Y/R of octagon shape and magnitude of load (a) 535.4 N (b) 688.6 N (c) 841.6 N (d) 994.6 N.

to along the horizontal direction decreased as magnitude of force pressed at the top and bottom of PMMA increases. The transmission of force along horizontal direction depended on edge length from contact area. Transmission of force increased as straight edge length increased because the tension surface of high edge length can distribute of force in vertical direction more than low edge length of sample.

It was found that relative maximum number of fringe order depended on shape of sample. The relative maximum number of fringe order of square was less than octagon and dodecagon shape. Therefore, the transmission of force from position of X/R = 0 along the horizontal direction of square was more than dodecagon and octagon shape because of the difference of edge length of sample.

3.2 Effect of Length Edge of Sample with Stress Distribution

When the shape of dark band from center to the edge of sample in horizontal direction is considered, it was found that vertex of dark band curved into center of sample and dark band is straight line in the middle region between center to edge of sample and the shape of dark band is convex towards the edge of the sample. Figure 6.

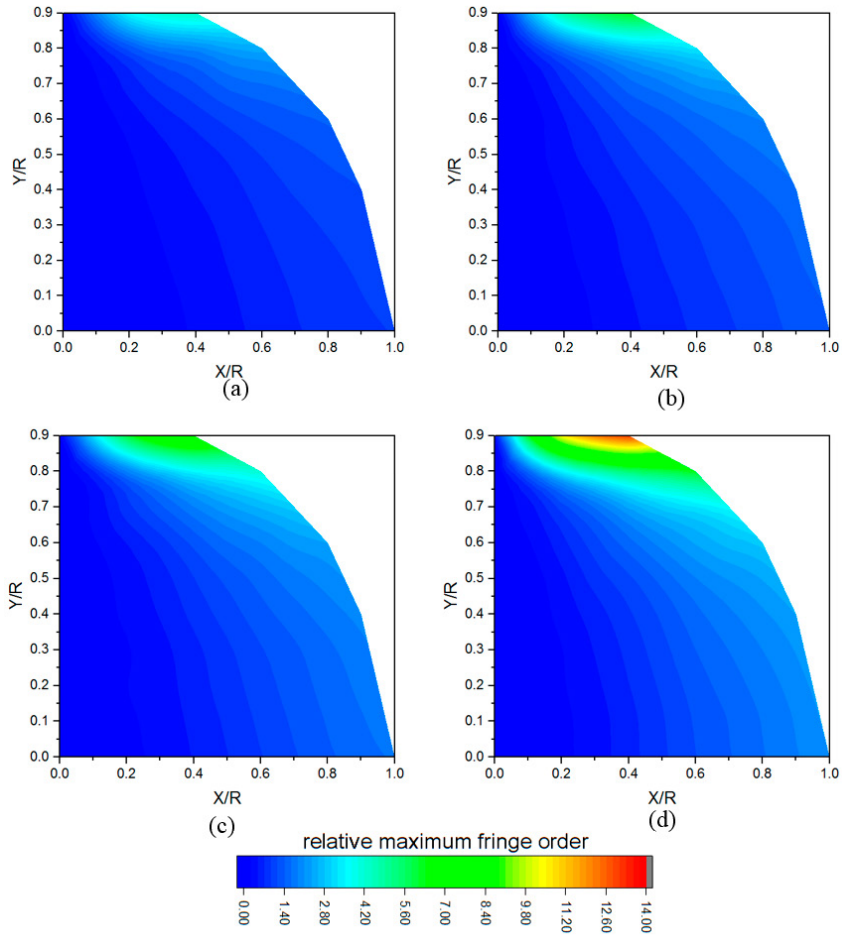

Figure 4. Relative maximum number of fringe order with X/R and Y/R of dodecagon shape and magnitude of load (a) 535.4 N (b) 688.6 N (c) 841.6 N (d) 994.6 N.

shows the isochromatic fringe order of square, octagon, dodecagon and circular disk [13,15-16]. It was found that the maximum fringe order of square, octagon, dodecagon and circular disk shape of PMMA was at the top of sample and decreased from the top to center and edge of sample in vertical and horizontal direction. The distribution of dark band produced at the first straight edge from contact area of sample of square, octagon and dodecagon shape as shown in Figures. 6 (a) - (d).

After calculating, the high number of fringe order (green, yellow and red area) is at y/R = 0.50-0.90 in vertical direction and x/R = 0.00-0.30 in horizontal direction of square shape. For octagon shape, the high number of fringe order is 0.55-0.90 in vertical direction and 0.00-0.25 in horizontal direction, the high number of fringe order is 0.65-0.90 in vertical direction and 0.00-0.20 in horizontal direction of dodecagon, the number of fringe order is at 0.45-0.90 in vertical direction and 0.00-0.20 in horizontal direction of circular disk as shown in Figures. 7 (a)-(d). The number of fringe order of square is more than octagon and dodecagon shape because the length of the first edge from contact area of loading square is more than octagon and dodecagon in Figures. 6 (a)-(b). So, the length of dark band of fringe of octagon

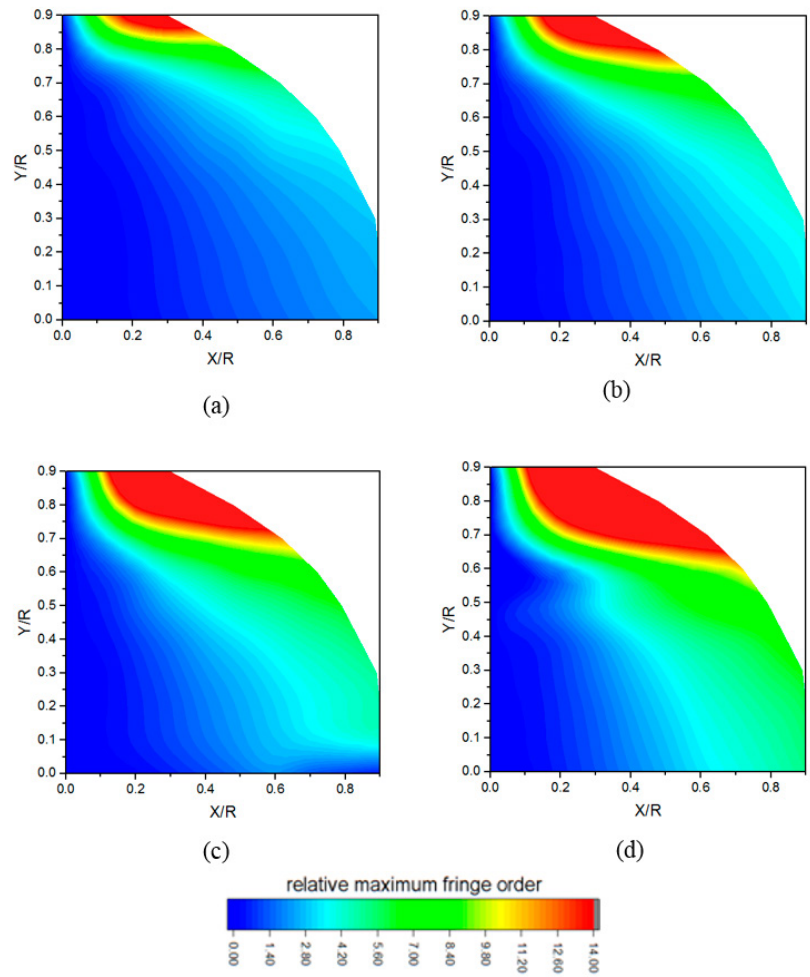

Figure 5. Relative maximum number of fringe order with X/R and Y/R of circular disk shape and magnitude of load (a) 535.4 N (b) 688.6 N (c) 841.6 N (d) 994.6 N.

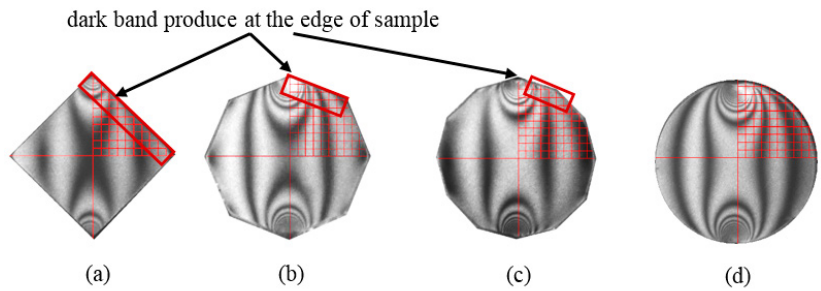

Figure 6. The dark band of isochromatic pattern at the first edge of (a) square (b) octagon (c) dodecagon shape and (d) circular disk.

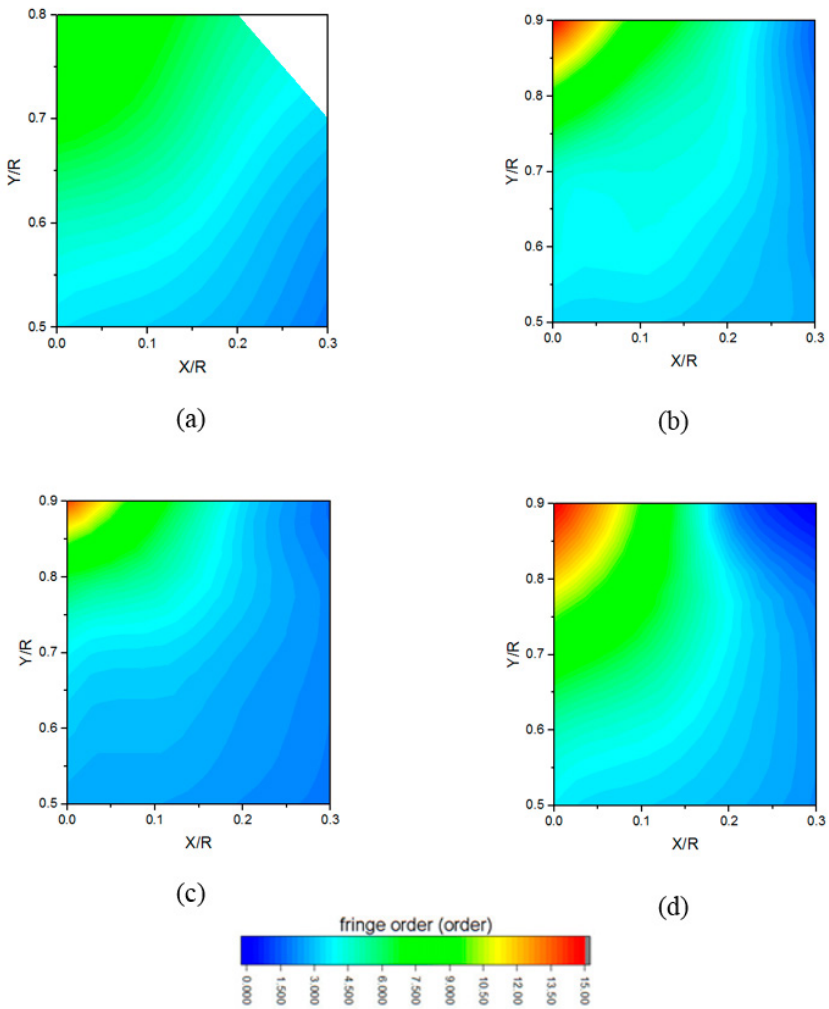

Figure 7. Isochromatic of fringe order (a) square (b) octagon (c) dodecagon (d) circular disk.

is more than dodecagon shape of PMMA and the transmission of force from contact area at top of sample of circular disk was more than octagon and dodecagon shape.

The length of edge decreased from octagon to dodecagon and then the curve edge of circular disk. It was found that the number of fringe order depended on length of edge of sample. The distribution of fringe order was related to the transmission of force from contact area at top of sample into every point of sample. Figures 7 (a)-(c) show the fringe order in each case. The high value of fringe order in vertical direction X/R = 0 and Y/R = 0.9 of circular disk was more than octagon and dodecagon shape. Therefore, the transmission of force in vertical direction at X/R=0 of circular disk was more than octagon and dodecagon shape because of the difference of edge length of sample. Moreover, high fringe order distributed from center to horizontal direction of octagon was more than dodecagon and disk because of the longer edge length of octagon shape.

4. Conclusions

In this experiment, PMMA was pressed by two-point load. The isochromatic patterns could be observed in every area of PMMA. The dark band could be observed at the edge of first straight edge of square, octagon and dodecagon shape. The relative maximum number of fringe order indicated the stress distribution in the sample. It was found that the transmission of stress in horizontal direction of square was more than octagon and then dodecagon. When the magnitude of force was increased from 535.37 to 994.63 N, the increasing of stress was at slower rate from center to the edge of PMMA.

The net fringe order depended on shape of PMMA where the dark band could be observed at the edge of square, octagon and dodecagon shape. The height of isochromatic fringe order in vertical direction of disk was more than square more than octagon and dodecagon. It depended on edge length from contact area of sample.

Acknowledgments

This research was also supported by the Faculty of Science at Sriracha, Kasetsart University Si Racha Campus for financial support. The authors are thankful to Chiang Mai University for facility supports.

References

[1] Peral D., Correa C., Diaz M., Porro J.A., Vicente J.D. and Ocana J.L., *Mater. Des.,* 2017; **132**: 302-313. DOI 10.1016/j.matdes.2017.06.051.

[2] Ajovalasit A., Petrucci G. and Scafidi M., *Opt. Laser. Eng.*, 2015; **68**: 58-73. DOI 10.1016/j.optlaseng.2014.12.008.

[3] Hariprasad M.P. and Ramesh K., *Opt. Laser. Eng.,* 2018; **105**: 86-92. DOI 10.1016/j.optlaseng.2018.01.005.

[4] Shang W., Ji X. and Yang X., *Optik,* 2015; **126**: 1981-1985. DOI 10.1016/j.ijleo.2015.05.053.

[5] Frankovsky P., Zubko P., Ostertag O., Papacz W. and Smida M., *Am. J. Mech. Mater.,* 2013; **1**: 329-334. DOI 10.12691/ajme-2-7-11.

[6] Kostkan J., Frankovsky P., Pastor M., Trebuna F. and Simcak S., *Procedia Engineering,* 2014; **96**: 235-241. DOI 10.1016/j.proeng.2014.12.149.

[7] Prasath R.G.R., Newton T. and Danyluk S., *Manuf. Lett.,* 2018; **15**: 9-13. DOI 10.1016/j.mfglet.2017.12.010.

[8] Kale S. and Ramesh K., *Opt. Laser. Eng.,* 2013; **51**: 592-599. DOI 10.1016/j.optlaseng.2012.12.013.

[9] Sun F., Lan T. and Pan X., *Opt. Laser. Eng.,* 2015; **74**: 87-93. DOI 10.1016/j.optlaseng.2015.05.010.

[10] Ali U., Juhanni K. and Buang N.A., *Polym. Rev.,* 2015; **55**: 678-705. DOI 10.1080/15583724.2015.1031377.

[11] Manjit Y., Limpichaipanit A. and Ngamjarurojana A., *Proc. SPIE,* 2018; **10714:** 107140D-6 . DOI 10.1117/12.2299637.

[12] Zandman F., S. Redner and Dally J.W., *Photoelastic Coatings,* Ames, Iowa: Iowa State University Press, 1977.

[13] Manjit Y., Limpichaipanit A. and Ngamjarurojana A., *Chiang Mai J. Sci.,* 2019; **46:** 787-798.

[14] Blicblau A.S., Singh M., McConnell E. and Pleaner M., *Math. Comput. Model.,* 2008; **47**: 1108-116. DOI 10.1016/j.mcm.2007.04.021.

[15] Jiang Y., Herrmann H.J. and Marroquin F.A., *Comput. Geotech.*, 2019; **113:** 103087. DOI 10.1016/j.compgeo.2019.05.002.

[16] Lu J., *Comput. Method Appl. Mat.,* 2009; **198**: 2391-2402. DOI 10.1016/j.cma.2009.02.029.